

# Scour at the Seawall in Surfside, Texas, During Hurricane Harvey (2017)

Nina Stark, Associate Professor, Virginia Tech, Blacksburg, VA, USA; email: <a href="mailto:ninas@vt.edu">ninas@vt.edu</a>
Iman Shafii, Ph.D. Candidate, Texas A&M University, College Station, TX, USA; email: <a href="mailto:ishafii@tamu.edu">ishafii@tamu.edu</a>
Navid Jafari, Assistant Professor, Louisiana State University, Baton Rouge, LA, USA; email: <a href="mailto:njafari@lsu.edu">njafari@lsu.edu</a>
Nadarajah Ravichandran, Associate Professor, Clemson University, Clemson, SC, USA; email: <a href="mailto:nravic@clemson.edu">nravic@clemson.edu</a>

Jens Figlus, Associate Professor, Texas A&M University, Galveston, TX, USA; email: figlusj@tamu.edu Stephanie M. Smallegan, Assistant Professor, University of South Alabama, Mobile, AL, USA; email: <a href="mailto:ssmallegan@southalabama.edu">ssmallegan@southalabama.edu</a>

**Patrick Bassal**, Geotechnical Engineer, WSP USA, New York, NY, USA; now at: Patrick Bassal; email: <a href="mailto:pcbassal@ucdavis.edu">pcbassal@ucdavis.edu</a>.

ABSTRACT: Hurricane Harvey was a Category 4 hurricane on the Saffir-Simpson hurricane wind scale. National Oceanic and Atmospheric Administration (NOAA) water level gages documented 1.1 m of water level elevation over predicted tide in Freeport, Texas, on 25 – 26 August 2017. The NOAA wave buoy 42019 offshore off Freeport documented wave heights > 7 m. A reconnaissance team of the Geotechnical Extreme Events Reconnaissance (GEER) Association visited Surfside, Texas, on 3 September 2017. While no significant damage to infrastructure was observed, the GEER team identified a significant scour runnel parallel to the Surfside seawall. The purpose of this article is to present the detailed observations of the scour runnel parallel to the Surfside seawall during Hurricane Harvey (2017). The sloped seawall is separating a shore-parallel street from the beach and is composed of angular boulders of approximately 30-50 cm in diameter. The observed runnel represented a depression of up to ~ 0.3 m in depth and ~ 4 m in width. It maintained mostly a distance of 0-5 m from the visible toe of the seawall. Boulders seemed particularly misplaced where the runnel approached the seawall. Sediments at Surfside Beach, Texas, are predominantly clean sands. During a second site visit by the members of the initial team in May 2018, no runnel was observed.

**KEYWORDS:** Hurricane Harvey, river line, embankment, erosion, storm damage

**SITE LOCATION: Geo-Database** 

# INTRODUCTION

Scour at seawalls is a well-known risk for coastal communities relying on the protection from ocean waves by a seawall (CIRIA 1986). Seawall damages in response to scour include loss of fill material, collapse, and breaching (Powell 1987). Sumer and Fredsoe (2002) list different scenarios impacting the mechanics of scour at a seawall. They distinguish between 2-D scenarios (waves break in front of seawall; waves break on seawall; waves are reflected without breaking; waves overtop seawall), and 3-D scenarios considering obliquely incident waves with generation of longshore currents or steady streaming and potential longshore currents generated by tides. Factors governing the development of scour are the location (i.e., water depth) and the type of seawall (e.g., vertical or sloped rubble-mound), wave breaking, sediment properties, and wave-seabed interaction (i.e., wave boundary layer mechanics). With regard to the latter, the wave loading may also induce soil liquefaction that may result in an increased erodibility of sediments (Kramer 1988; Tsai 1995; Sumer and Fredsoe 2002; Whitehouse 2006).

Most studies associated with scour at seawalls are based on laboratory experiments (e.g., Fowler 1992, Sumer and Fredsoe 2000, Figlus et al. 2011). Few documented case studies and field observations are currently available in the literature.

Submitted: 14 August 2018; Published: 2 July 2020

Reference: Stark N., Shafii I., Jafari N., Ravichandran N., Figlus J., Smallegan S. M., and Bassal P. (2020). Scour at the Seawall in Surfside, Texas, During Hurricane Harvey (2017). International Journal of Geoengineering Case Histories, Volume 5, Issue 4, pp. 62-76, doi: 10.4417/IJGCH-05-04-04



Particularly, observations after severe storm events are rare, in part due to the ephemeral nature of the scour feature, highlighting the need for immediate reconnaissance after (or even during) the storm event to document scour prior to infilling when the hydrodynamic conditions have calmed down. More recent examples associated with scour in front of a buried seawall in New Jersey during Hurricane Sandy (Nederhoff et al. 2015), or associated with the Gold Coast seawall, Australia (Tomlinson et al. 2016), have been documented. Nevertheless, more observations after extreme events are needed to better understand infrastructure response to scour formation.

Studies on scour at seawalls are reported in the literature, including Herbich and Ko (1968), Kraus and McDougal (1996), Tsai et al. (2009), and Carley et al. (2015). Most studies aim for the development of methods and expressions for scour prediction and simulation. For example, Fowler (1992) proposed an expression (Equation 1) to predict scour depth S in front of a vertical seawall. Fowler (1992) related the dimensionless ratio of scour depth and significant wave height  $H_0$  to the water depth at the wall  $h_w$ , and the deep-water wave length  $L_0$  from empirical testing (Fig. 1):

$$\frac{S}{H_0} = \left(22.75 \frac{h_W}{L_0} + 0.25\right)^{\frac{1}{2}} \tag{1}$$

Figure 1 introduces the general parameters used. In that regard, the significant wave height  $H_0$  can be approximated as the mean of the highest third of the measured wave heights H. The deep water wave length  $L_0$  represents the wave length L far enough offshore where water depths are deep enough that the wave shape and characteristics (including length) are not impacted by interaction with the seabed. Sediment properties are not considered in this expression. Later, McDougall et al. (1996) derived an expression (Equation 2) including grain size d (or an available and suitable representation, if applicable, such as median grain size) and beach slope m from numerical simulations:

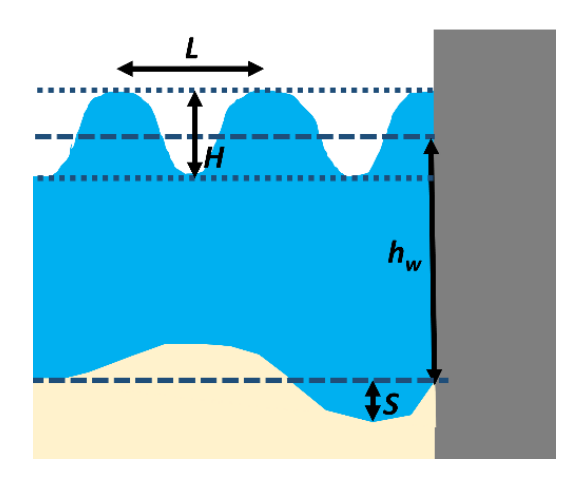


Figure 1. Schematic drawing of a vertical seawall (grey), seabed (beige), and water conditions (blue) introducing relevant symbols: scour depth in front of the seawall S, still water depth at the seawall S, wave length S, and wave height S.

$$\frac{S}{H_0} = 0.41 m^{0.85} \left(\frac{L_0}{H_0}\right)^{0.2} \left(\frac{h_w}{H_0}\right)^{0.25} \left(\frac{H_0}{d}\right)^{0.33} \tag{2}$$

Equations 1 and 2 were developed for breaking waves and vertical seawalls. For sloping rubble-mound seawalls, scour is expected to be less significant for the same wave conditions. This results from the sloping seawall face, as well as from porosity of the seawall (Sumer and Fredsoe 2002). For larger water depths in which waves may not break, but are reflected from the seawall, scour is reduced with increasing water depths relative to the wave length. Wave overtopping may also lead to a significant scour at the toe of the seawall resulting from the jet and turbulence of the backflow. However, Figlus et al. (2011) demonstrated that overtopping and overwash can in some cases also reduce scour. Another aspect that may increase the scour is longshore currents that may be superimposed to the waves, or may be generated by obliquely incident waves (Sumer and Fredsoe 2002).

Hurricane Harvey was a Category 4 hurricane on the Saffir-Simpson hurricane wind scale. National Oceanic and Atmospheric Administration (NOAA) water level gages documented 1.1 m of water level elevation over predicted tide in Freeport, Texas,



on 25 – 26 August 2017. The NOAA wave buoy 42019 offshore off Freeport documented wave heights > 7 m. A team from the Geotechnical Extreme Events Reconnaissance (GEER) Association visited Surfside Beach, Texas, on 3 September 2017 at around 20:00 UTC, approximately 8 days and 17 hours after Hurricane Harvey's first landfall near Rockport, Texas (about 200 km southwest of Surfside Beach). Hurricane and Tropical Storm warnings continued through 31 August 2017 for the Surfside Beach area. The team visited an approximately 0.75 km long stretch of Surfside Beach reaching from N28°56′46.22″ W95°17′18.44″ southwest to N28°56′27.30″ W95°17′34.97″, and observed a ridge-runnel geomorphology in front of the Surfside Beach's sloped rubble-mound seawall (Stark et al. 2017). Local residents confirmed that this beach morphology formed during Hurricane Harvey. Furthermore, dislocated boulders were found that may also have shifted in response to wave forcing and/or sediment erosion. Members of the same team revisited the location on 9 May 2018 and found no ridge-runnel formation.

This article presents observations and an associated limited analysis of scour at the sloped rubble-mound seawall in Surfside Beach, Texas, during Hurricane Harvey, following the site reconnaissance by the GEER Hurricane Harvey South team (Stark et al. 2017). The observations were discussed in the context of two simple and conservative expressions by Fowler (1992) and McDougall et al. (1996) to estimate scour in front of a vertical seawall with breaking waves, as well as a simple approach by Sumer and Fredsoe (2000) for sloped rubble mound seawalls. This represents a unique case study of scour observations in front of a sloped rubble-mound seawall during a Category 4 (Saffir-Simpson scale) hurricane. A brief background on the local geology and oceanographic conditions relevant for sediment transport processes, as well as on the construction activities associated with Surfside Beach's seawall, are provided in the next section

# REGIONAL CONTEXT

This section provides a brief background on the local geology and oceanographic conditions relevant for sediment transport processes, as well as on the remedial activities associated with Surfside Beach's seawall. Surfside Beach (Fig. 2) is located in Brazoria County, fringes the Gulf of Mexico, and is home to a population of about 500 people. Prior to the Brazos River diversion by the U.S. Army Corps of Engineers in 1929, the Brazos Delta was located adjacent to the study site to the West (Seelig and Sorensen 1973). The old delta was about 30-35 km² in area, and extended to a water depth of about 20 m. The delta was asymmetric to the West, and has been significantly reworked by currents and waves (Rodriguez et al. 2000). Sediment cores collected prior to the 1992 flood event showed that the old Brazos delta area features a surficial layer of shoreface sands interbedded with mud and muddy sands. Rodriguez et al. (2000) described the sands as well-matured with rounded to subrounded, well-sorted particles with grain sizes ranging from about 0.08-0.1 mm and scattered shell fragments. This surface layer is underlain by clayey prodelta sediments and pleistocene clay (Rodriguez et al. 2000).

Snedden et al. (1988) investigated the transport mechanisms of the thin surficial sand layers on the central Texas shelf. During fair-weather conditions, they observed near-bottom flow velocities of 0.1-0.2 m/s at water depths of ~ 12 m, and deep water waves of up to ~ 1 m with wave periods of 5-6 s. They concluded that those flow conditions did not exceed thresholds for sand transport during most of the fair-weather times. If the threshold was exceeded, onshore-directed and longshore sediment transport were most likely. During storm conditions, near-bottom and nearshore current speeds were in excess of 40 cm/s, and offshore wave conditions featured wave heights of 2 m with 9 s wave periods (Snedden et al. 1988). During Hurricane Andrew in 1992, significant wave heights of ~ 9 m were recorded offshore of Corpus Christi, Texas, but did not exceed 1.5 m off Freeport (DiMarco et al. 1995). During Tropical Storm Bill in 2015, significant wave heights of almost 2 m, near-bottom current velocities of up to approximnately 35 cm/s, and peak suspended sediment concentrations of 8.56 g/l with offshore directed sediment transport were reported in the region (Frost 2015).

Watson (2003) concluded that Surfside Beach was experiencing significant and increasing erosion associated with construction activities and diversion of the Brazos River and ongoing developments of long jetties and a deep channel for the Freeport Harbor entrance. The same author also highlighted that the areas provided little sediment sources to sustain frequent beach nourishment. Additionally, groundwater extraction and associated subsidence were identified as a cause of shoreline retreat. Watson (2003) concluded that beach erosion at Surfside Beach could only be significantly reduced by continuing beach nourishments and/or armoring of the shoreline with a seawall. In August 2007, a final environmental assessment of the "Surfside Beach Shoreline Protection Project" was prepared by TCB Inc. in Austin, Texas, for the Federal Emergency Management Agency (FEMA), proposing a revetment for Surfside Beach. In 2008, the revetment or sloped rubble-mound seawall was constructed along Beach Drive just prior to Hurricane Ike. During Hurricane Ike, the seawall experienced severe damage according to Coast & Harbor Engineering (http://www.coastharboreng.com), leading to further assessment, repair,



and enhancement of the structure as well as beach nourishment with  $\sim 140,000$  cubic yards of sand in 2011 (TXGLO 2019). The repairs and enhancement included replacement of the existing armor stone along the crest by granite stone blocks, and reinforcement of the structure slope by placement of the previous crest stones. More details on this can be found in Connor et al. (2017).

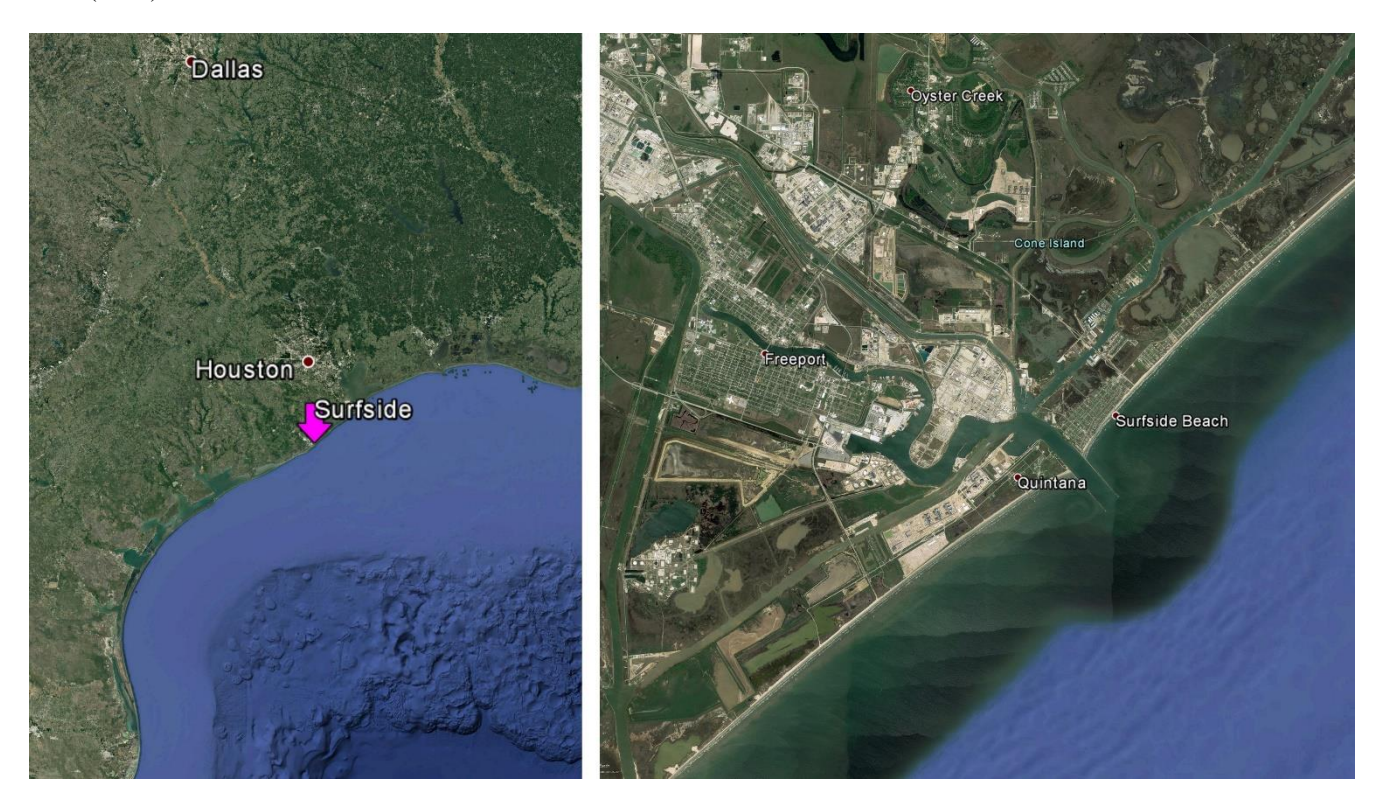


Figure 2. Google Earth images (Google Earth 2018) of Surfside Beach, TX, in the context of the Gulf of Mexico (left) and in the context of the Freeport region (right).

# **RESULTS**

The following types of data were analyzed for this study: metocean data from public sources, observations by the GEER team, sediment samples collected by the GEER team, and high-resolution pan-sharpened satellite imagery. The data are organized in respective sections.

# Weather and Hydrodynamic Conditions

Hurricane Harvey made landfall east of Rockport, Texas, on 25 August 2018, (yearday 237; i.e., day 237 of the year) with estimated sustained wind speeds of about 60 m/s (Blake and Zelinsky 2018). Figure 3 shows the wind data collected at NOAA (National Oceanic and Atmospheric Administration) station FPST2 (8772471) close to Freeport. Wind speeds approximately two weeks before and after Hurricane Harvey's landfall in Texas ranged from phases of approximately 3 m/s to about 8 m/s, and increased rapidly with the approach of Hurricane Harvey. No wind speeds were measured during the hurricane impact on this area and at this station. However, the wind direction developed from approximately 80° (approximately from the East) to approximately 180° (from the South) from yearday 237-246. Wind speeds stabilized to mostly < 5 m/s on yearday 243.

Measured water levels matched the tidal predictions reasonably well up to yearday 236 (Fig. 4). Neap tide conditions with water elevation fluctuating from about 0.2-0.45 m from mean lower low water were predicted for yeardays 236-238. However, the water levels reached up to about 1.3 m on yearday 237 and up to 1 m until yearday 242. Water levels were measured ~ 0.2 m lower than predicted values on yeardays 243-244 before approaching predicted values again. Another phase of elevated water levels in the same month was observed from yearday 251-255 with a water levels being elevated by about 0.3 m



compared to the predicted values. The station is located in the Freeport port entrance in a small embayment on the Surfside Beach side. Effects of the embayment and entrance morphology on the measurements in comparison to the open ocean front of Surfside Beach must be considered.

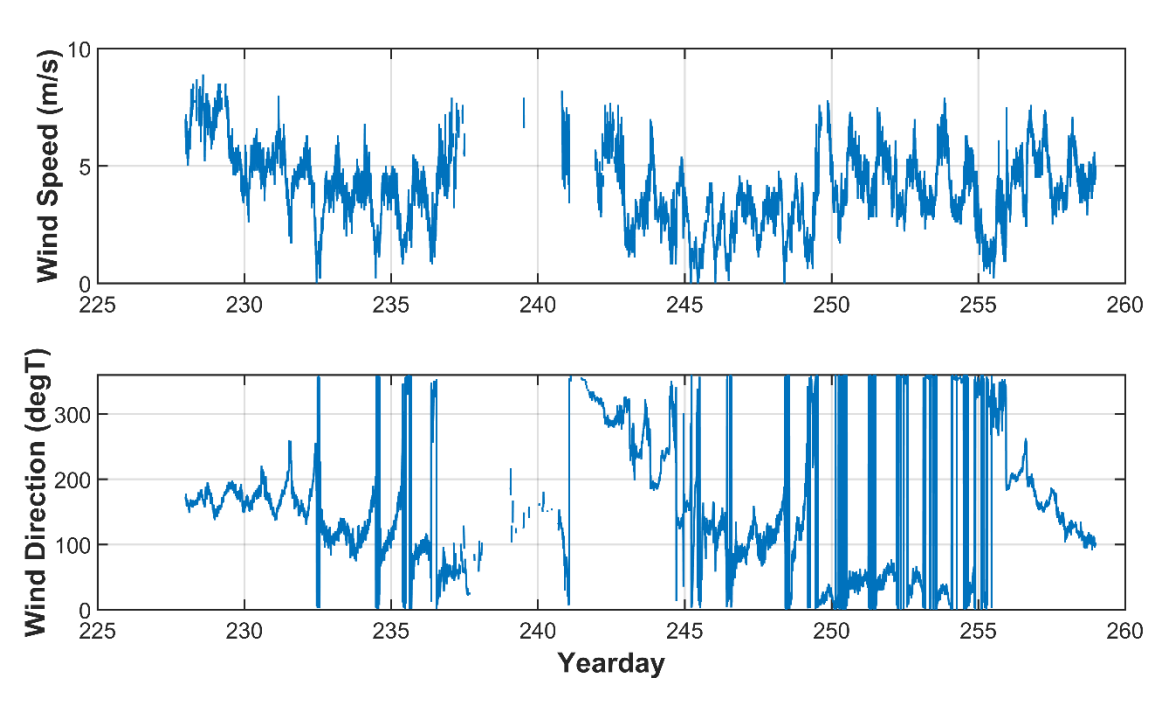


Figure 3. Recordings of wind speed (m/s) and wind direction (degrees from true North) from NOAA station FPST2 (8772471) close to Freeport, Texas, (28.936°N 95.294°W) from 16 August (yearday 228) to 15 September 2017 (yearday 258; landfall of Hurricane Harvey close to Rockport occurred on yearday 237).

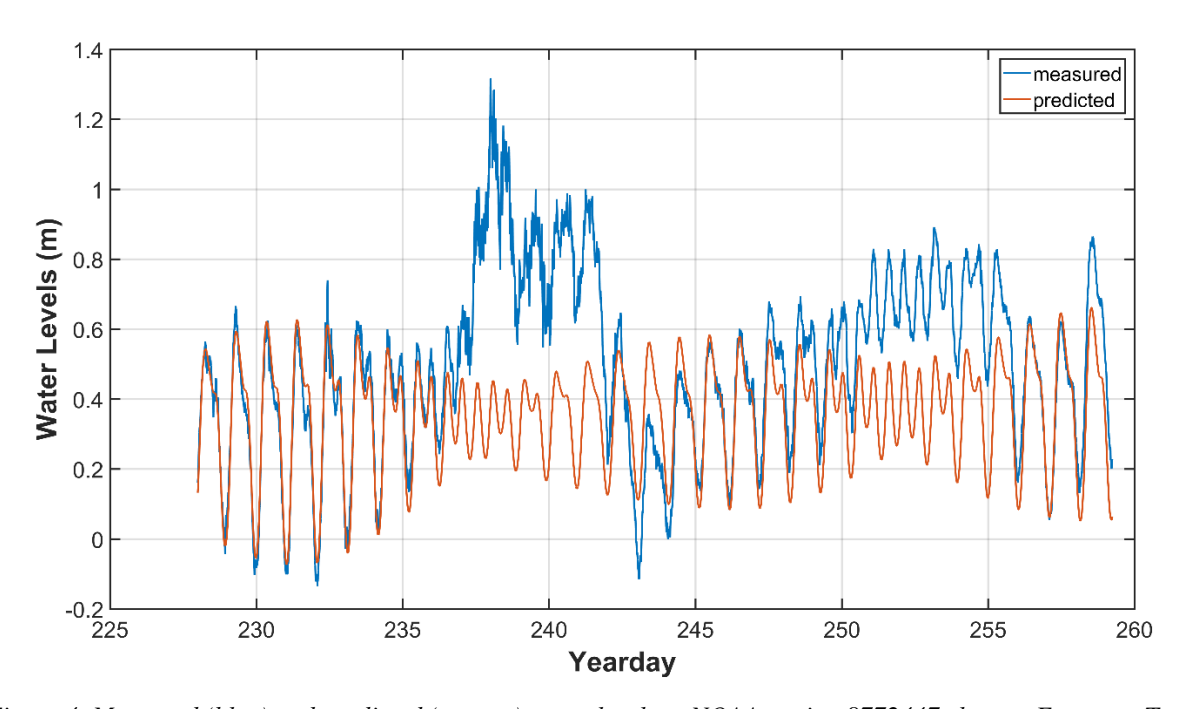


Figure 4. Measured (blue) and predicted (orange) water levels at NOAA station 8772447 close to Freeport, Texas, (28.943°N 95.302°W) from 16 August 2017 (yearday 228) to 15 September 2017 (yearday 258). The water levels are displayed in relation to mean lower low water (average of the lower low water height observed over the U.S. National Tidal Datum Epoch (NOAA 2019).



Wave data were collected at NOAA station 42019 (LLNR 1205), being located 60 nautical miles south of Freeport at a water depth of  $\sim$  82 m (Fig. 5). The measured values can be considered deep-water conditions. Wave heights were generally low in the investigated month with significant offshore wave heights mostly < 2 m, and wave periods  $\sim$  5.5 s. On yearday 238, significant wave heights of  $\sim$  7m with dominant wave periods of  $\sim$  11 s were recorded, followed by significant wave heights of 2-4 m with dominant wave periods of 7-9 s until yearday 243. Waves came mostly from the South ( $\sim$  180°) during the event, and turned to the opposite direction toward the end of the wave event.

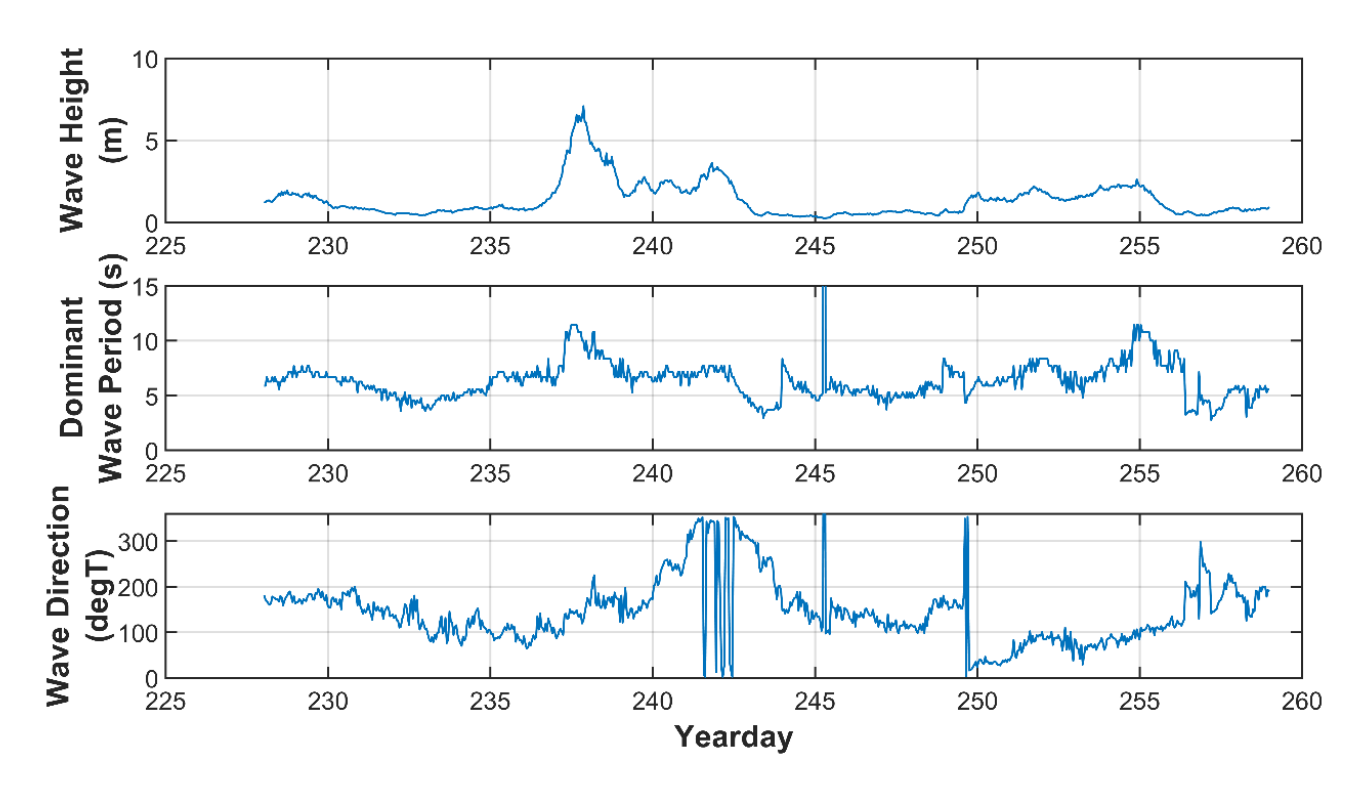


Figure 5. Significant wave heights (top panel), dominant wave periods (center panel), and wave direction (bottom panel) at NOAA station 42019 south of Freeport, Texas, (28.907°N 95.359°W) from 16 August 2017 (yearday 228) to 15 September 2017 (yearday 258).

# **GEER Team Observations**

Members of the GEER team visited Surfside Beach on yearday 246 at approximately 20:00 UTC (Stark et al. 2017). At the time of the visit, the beach was again utilized by tourists and local residents. Minor observable damage to the seawall or infrastructure was documented by the GEER team, which is in line with assessments and opinions of local residents. However, a well-formed runnel of about 20-40 cm depth had formed approximately seawall-parallel (Figs. 6 and 7). Local residents confirmed that this runnel had formed during Hurricane Harvey. The runnel was fringed by rather sharp edges with the offshore directed edge being overall less steep than the onshore directed edge. The runnel width varied from about 1.5-4 m. The narrower sections were typically closer to the seawall toe (Fig. 6 lower left). In some sections, the onshore edge of the runnel was located at a distance about 2-3 m from the toe of the seawall. In these cases, the beach between the runnel and the seawall toe appeared fairly steep (Fig. 6 lower right). Dislocated boulders from the seawall were found, and seemed to be predominantly co-located with sections where the runnel approached the seawall toe (Fig. 6 left). Offshore of the runnel, a rather flat ridge of about 15-25 m width was observed (Fig. 6 right). The slope of this ridge was clearly flatter than the slope of the beach between the runnel and the seawall (if present).





Figure 6. Seawall-beach-runnel-ridge system observed on yearday 246 at approximately 20:00 UTC (15:00 local time) at Surfside Beach, Texas. The following coordinates represent the position of the photographer for each image: A) and B) 28.9433°N 95.2920°W, C) 28.9434°N 95.2918°W, D) 28.9461°N 95.2890°W.



Figure 7. Seawall-beach-runnel-ridge system observed on yearday 246 at approximately 20:00 UTC (15:00 local time) at Surfside Beach, Texas. The following coordinates represent the position of the photographer for each image: A) 28.9460°N 95.2890°W, B) 28.9451°N 95.2903°W.

Small waves approached the beach at the time of the visit (Fig. 7 right). Offshore significant wave heights on that day were less than 0.5 m (Fig. 4). These small waves were visibly breaking at the offshore side of the flat ridge (Fig. 6 right) with a



swash bore running over the ridge and into the runnel (Fig. 6 right, Fig. 7). Wave reflection within the runnel seemed apparent, and little to no swash was observed at the onshore runnel edge (Figs. 6 and 7).

At the offshore runnel edge, a significant amount of sediment transport was observed, and recorded in an underwater video. Sand was mobilized from the edge and carried into the runnel, likely actively infilling the runnel, and decreasing the height of the ridge. This observation was also expressed in a sediment cloud and murkiness of water at the offshore runnel edge in Figure 6 (lower right).

A conceptual sketch of observations is provided in Figure 8. Overall, the runnel appeared to have formed through scour, which was driven by breaking or reflected waves from the seawall. It should be mentioned that the tidal level at the time of the observations was approximately 0.4 m above mean lower low water based on NOAA gage 8772447. This means that during Hurricane Harvey local water levels may have been up to 90 cm higher, submerging the beach entirely.

During a second site visit by members of the initial team in May 2018, no runnel was observed. However, displaced boulders were still visible, and an overall sediment accumulation was noted.

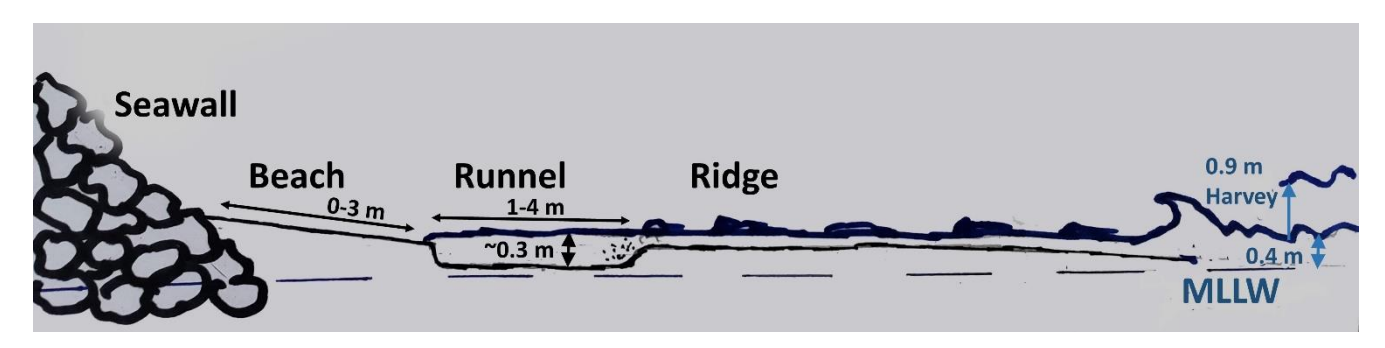


Figure 8. Conceptual sketch of observations by the GEER team at Surfside beach (yearday 246; 20:00 UTC).

# **Sediment Sampling**

The GEER team collected three disturbed and surficial sediment samples at Surfside Beach on yearday 246. Samples were collected using a small shovel and were deposited in sample bags. The respective samples represent locations on the beach, the runnel, and the ridge. No significant differences in sediment type were observed between the samples. Overall, the sediment samples exhibited a median grain size of  $d_{50}$ = 0.2 mm with 99.8% of sand content. The coefficient of curverture  $C_c$  equalled 1.07, and the coefficient of uniformity  $C_u$  equalled 2.1. According to the Unified Soil Classification System (USCS) the sediment classifies as poorly graded sand (SP). After the Wentworth (1922) scale, the sediment classifies as fine sand.

The samples were remolded in the soil erosion laboratory at Texas A&M University. The samples were compacted in three equal layers in Shelby Tubes using a standard compaction hammer to achieve a minimum of 18 kN/m³ total unit weight. Erosion Function Apparatus (EFA) tests were performed on each of the samples to investigate the erodibility of the material following the procedure outlined in Briaud (2001) and Briaud et al. (2017). The EFA measures the relationship between the erosion rate, water velocity, and hydraulic shear stress at the soil-water interface. Erosion rate was measured in terms of mm of sample height per hour for flow velocities of 0.306 m/s, 0.438 m/s, and 0.691 m/s, corresponding to shear stresses of 0.339 Pa, 0.672 Pa, and 1.55 Pa, respectively. Results for all three samples are shown in Figure 9, classifying the samples at the border of very highly erodible to highly erodible.

#### **Satellite Imagery**

Satellite imagery was obtained from Google Earth from 21 November 2015, 22 January 2017, and 21 March 2018 (Fig. 10). All of these dates are well prior to or post Hurricane Harvey and, therefore, represent conditions mostly unrelated to Hurricane Harvey. Even conditions in March 2018 are likely minorly affected by Hurricane Harvey, as no major damage to the seawall, significant net erosion, or major effects on local geomorphology can be identified in the image. The purpose of the presentation of these images is to provide a brief insight into general conditions at the site. In November 2015, wave action is present and visible. According to NOAA, offshore significant wave heights reached 0.8-3 m on the day of the image, with



a significant wave height of about 1.1 m at the time of the image. Crest-to-crest distances and wave lengths of the approaching waves were about 20 m from the satellite image. The width of a visible beach varied from about 0-18 m in front of the seawall and in the area of interest (Fig. 10). Wave breaking appears most prominent at the shoreline with the second line of waves breaking at a distance of ~ 85 m from the seawall. On 22 January 2017, wave conditions were calm.

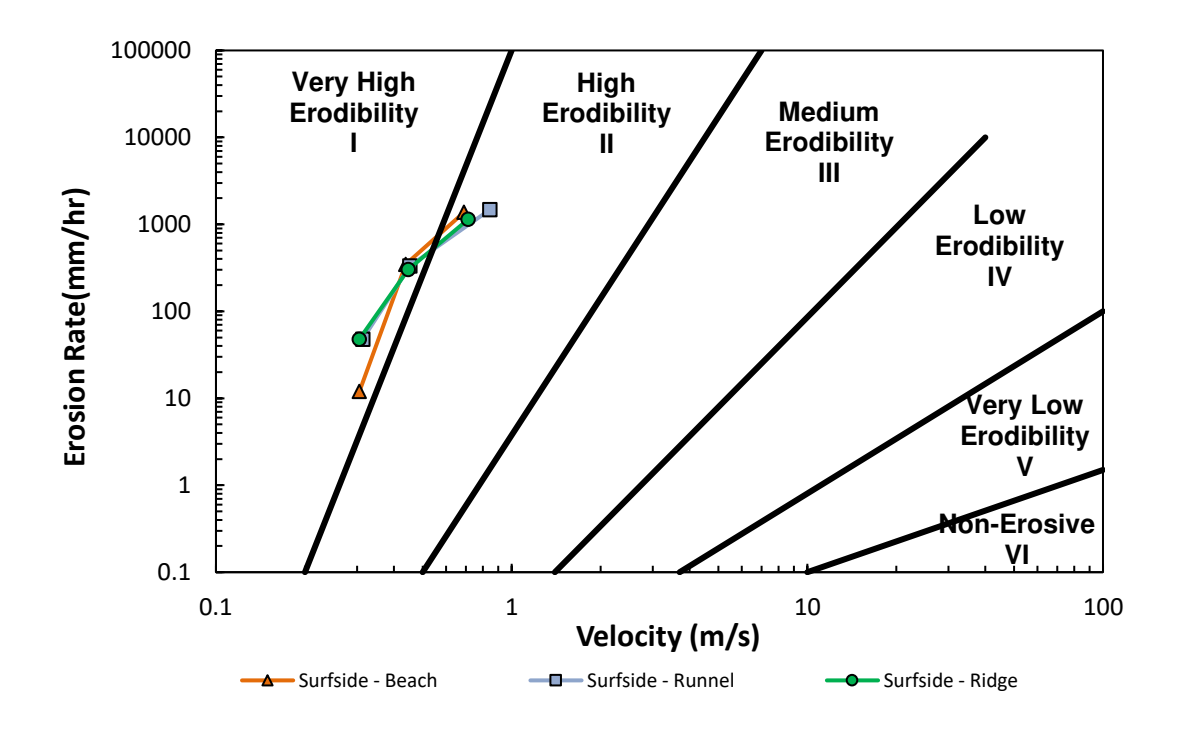


Figure 9. Summary of EFA test results.

A runnel system is clearly visible with beach widths from less than 2 m to 30 m, and associated variations in the position of the runnel. The runnel width varied similarly to the development of the runnel from less than a meter to about 10 m. It should be noted that wave conditions were overall rather energetic in this month, despite calm conditions at the time of the image. On 21 March 2018, waves were more visible in the image again, having crest-to-crest wave lengths of about 15 m in the area of interest in the image. The beach width reached from 5-20 m, and some wave breaking is visible at the shoreline, while dominant wave breaking occurred at a distance of ~ 60 m from the shoreline. It should be noted that water levels varied for the imagery. On 21 November 2015, water levels were about 0.75 m above mean lower low water at NOAA gage 8772447 at approximately noon local time (being a typical time for optical satellite imagery), and were about 30 cm higher than the predicted tide. On 22 January 2017 at noon local time, the actual water level was 0.12 m above mean lower low water, being about 10 cm lower than the predicted tide. On 21 March 2018 at noon local time, the actual water level was 0.34 m, being within 5 cm from the predicted values.

Figure 11 shows satellite images from yeardays 242 (30 August 2017), 245, and 248 during the Hurricane Harvey event. Only yearday 242 still featured elevated water levels in Freeport and somewhat larger offshore waves (Figs. 4 and 5). However, it should be noted that the measured offshore waves were mostly directed offshore at that time (Fig. 5). The satellite image from yearday 242 clearly shows a large amount of suspended sediments in the water. The beach width is narrow (0-7 m) in front of the seawall in the area of interest. It should furthermore be noted that a clearer morphology may not be visible due to the murkiness of the water from suspended sediments. The evolution of a thin runnel close to the seawall (0-4 m) and a partially less well-developed ridge appear visible. Some wave breaking is visible about 35 m from the seawall.

On yearday 245, the day prior to the visit of the GEER team, a well-defined ridge-runnel is visible with a beach width of 0-4 m, a runnel width of 3-10 m, and some wave breaking at the offshore edge of the ridge at a distance of  $\sim 25$  m from the seawall. Imagery may suggest a second ridge at a distance of  $\sim 50$  m from the offshore edge of the clearly visible ridge.



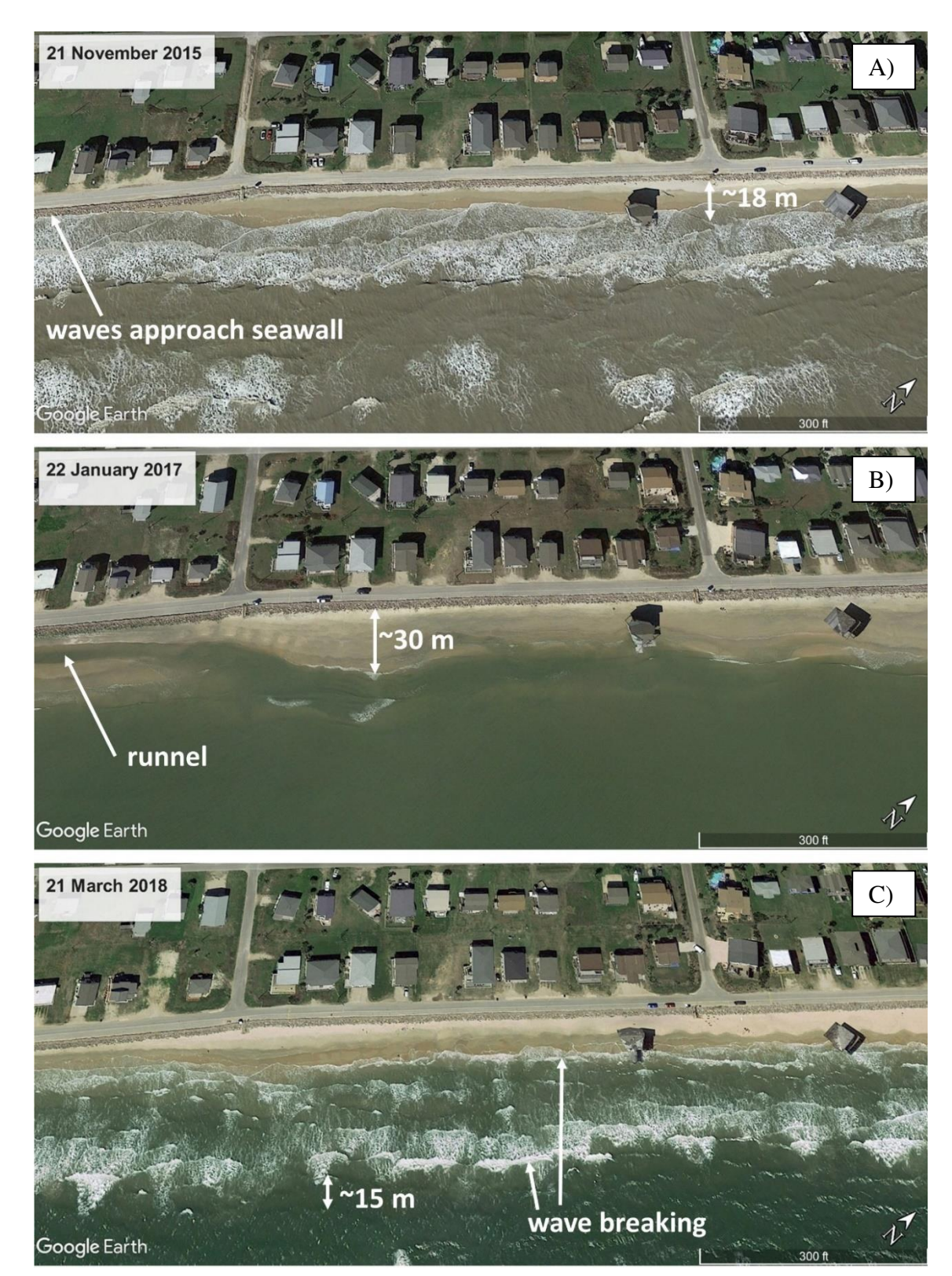


Figure 10. Google Earth satellite imagery from the area of interest at Surfside Beach well prior to and post Hurricane Harvey (Google Earth 2018a-c for panels A, B, and C, respectively).



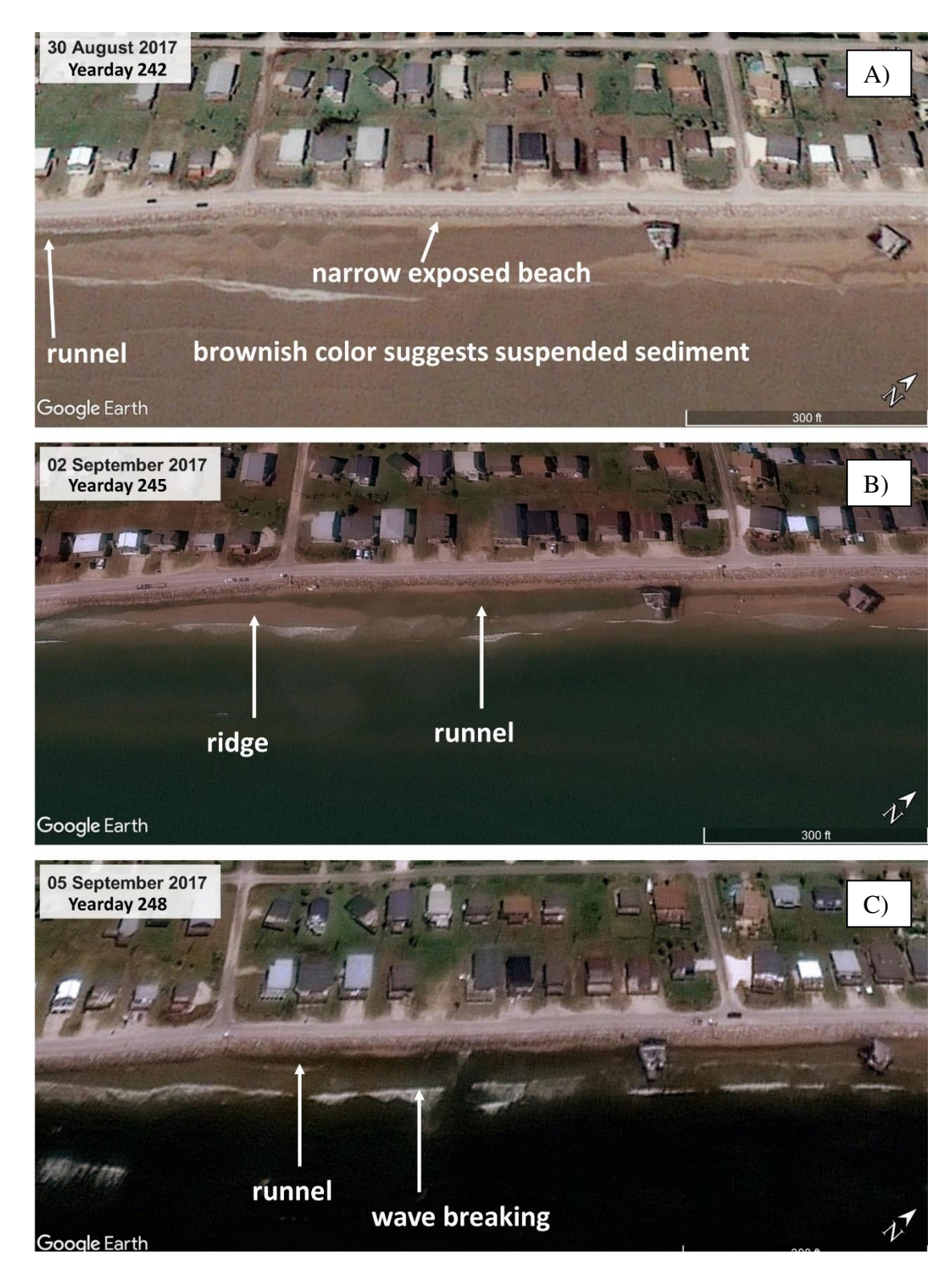


Figure 11. Satellite imagery from the area of interest at Surfside Beach. Images were displayed in Google Earth. Panel A) Yearday 242, collected by Pleiades 1 with an image resolution of 50 cm; Panel B) Yearday 245, collected by WorldView 3 with an image resolution of 30 cm; Panel C) Yearday 248, collected by WorldView 2 with an image resolution of 50 cm.



On yearday 248, the runnel is still visible. However, a decrease in width and a loss in height of the ridge seems to be indicated by the image. Again, assuming that imagery was collected around noon local time, some minor differences in water level must be expected (Fig. 4).

Figure 12 shows a satellite image from yearday 250, displaying clearly increased wave action. Nevertheless, the runnel seemed to be sustained during these wave conditions, and wave breaking closest to the shore appeared to occur along the previous location of the ridge. A second line of wave breaking appeared to be co-located with the previous second ridge. These observations may also be compared to the evolution and destruction of a shore-parallel bar system (e.g., as noted in Lippmann et al. 1989, Shand et al. 2001).



Figure 12. Satellite image from the area of interest collected on yearday 250 by KOMPSAT-2 with a resolution of 1 m.

# **Scour Analysis and Discussion**

Different mechanisms can lead to the development of the observed scour pattern. Assuming that longshore variability of the observed morphology was minor, the observations can be simplified to a two-dimensional beach-runnel-ridge system with potentially the formation of a second ridge. It may also be argued that this can be described as a nearshore sand bar system. However, the trough or runnel seems to be deeper and more developed than the accumulation of sediment at a well-defined narrow bar. For that reason, observations are considered rather indicative of a scour runnel-ridge system resulting from the interaction of waves with the seawall. The performed EFA tests clearly indicated that the abundant sediments are highly erodible and easily subject to erosion during an extreme event.

Sumer and Fredsoe (2002) depicted different flow processes leading to two-dimensional scour at seawalls: wave breaking near the wall, wave breaking on the wall, wave reflection, and overtopping of the seawall. News outlets presented video footage from Surfside Beach from yearday 237 with no visible overtopping of the seawall, but rather waves breaking offshore of the beach house structures (Fig. 13). While the video footage provided limited images of the beach, it suggested that wave breaking on the wall and overtopping of the seawall were unlikely. Even wave breaking near the seawall seems unlikely based on the video footage, the shallow water conditions, and an overall flat nearshore slope. Therefore, wave reflection after initial wave breaking may be a likely mechanism. Sumer and Fredsoe (2002) depicted that in the case of a rubble-mound breakwater and dominant bedload transport, sediment deposition (formation of a ridge) occurs at the nodes of a standing wave resulting from wave reflection. Nodes and antinodes (i.e., runnel and ridge) have a distance of a quarter of a wave length, and in the case of a sloped rubble-mound wall the first antinode in contact with the wall is practically located on the sloped surface of the seawall. This means the seawall slope impacts the location of the runnels and ridges. Furthermore, sediment suspension changes the organization pattern. However, dominant near-bed transport may be an acceptable assumption, considering the shallow water depth. Another impact on the ridge-runnel profile is wave irregularity, which also likely contributed to the longshore variability in addition to some minor local variations in seawall slope.





Figure 13. Screenshot from video footage from Surfside Beach on yearday 237 extracted and modified after Henry (2017).

A simple assessment of the central runnel to central ridge distance from the WorldView 2 image on yearday 245 was attempted, leading to an estimated distance of 7-12 m. Keeping in mind the irregularity of the waves and the fact that here the water depth is significantly smaller than the incident wave height, Sumer and Fredsoe (2000) suggested a rather distorted bed profile with a narrower and deeper runnel and wider ridge, which aligns with our observations.

Both scour assessment expressions shown in Equations 1 and 2 were tested. The following parameters were used:  $H_0$ = 7 m on yearday 238 and  $H_0$ = 3 m on yeardays 239-243; T= 11 s on yearday 238 and T= 8 s on yeardays 239-243;  $h_w$  ranging from 0.1-1.5 m, an estimated beach slope of 5°, and a grain size of 0.2 mm. The deep-water wave length was calculated using the dispersion relationship. Results using Equation 1 are shown in Figure 14. Figure 14 also depicts the relationship between  $h_w/L_0$  within the tested range of  $h_w$ , showing that the conditions lie within the applicable range of -0.011 <  $h_w/L_0$  < 0.045 for Equation 1 by Fowler (1992). The scour depth is clearly over-predicted (about ten times deeper than observed; Fig. 14 right). Equation 2 led to even larger over-predictions. This is not surprising, as these expressions were developed for vertical wall seawalls, breaking waves, and the associated scour at the seawall. Also, these expressions do not take into account the irregularity of the waves, amongst other limitations. Sumer and Fredsoe (2000) suggested a relationship between the angle of the sloped rubble-mound seawall, the ratio of water depth over wave length h/L, and the ratio of scour depth and wave height S/H. Assuming  $0.05 \le h/L \le 0.1$  (for example, 1 m in water depth and 20 m in wave length), and a slope of 30-40°, S/H equals 0.1-0.7. To generate a scour depth of 30 cm, wave heights between 0.4-7 m would be needed, being well within the possible range.

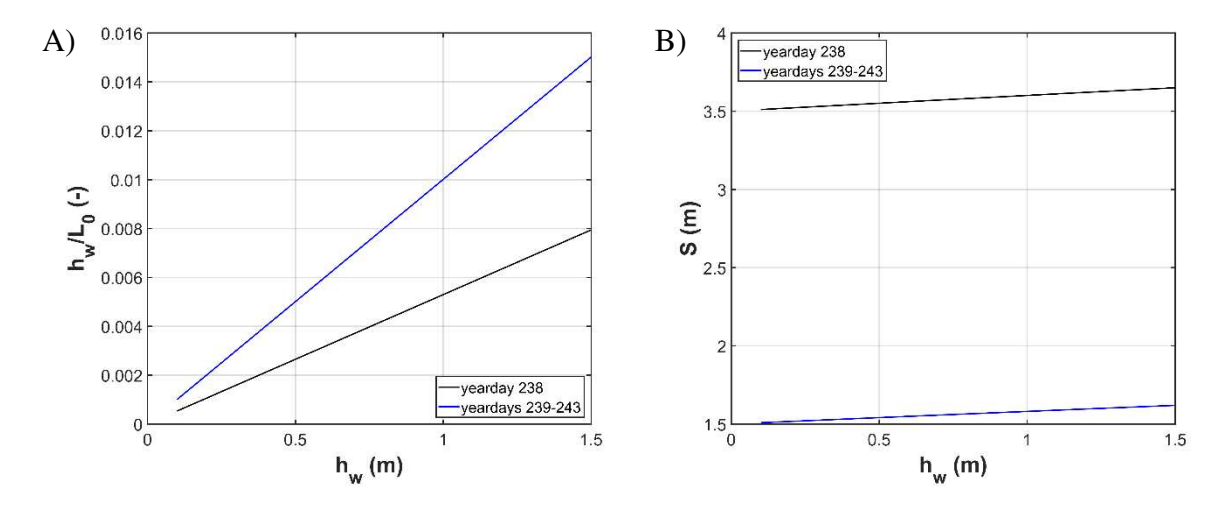


Figure 14. A) Water depth at the seawall  $h_w$  vs. the relationship between  $h_w$  and the deep water wave length  $L_0$  for conditions on yearday 238 (black) and yeardays 239-243 (blue). B) Estimated scour depths S within the same days and range of  $h_w$  after Equation 1 (Fowler 1992).



# **CONCLUSIONS**

Observations and a limited analysis of the beach morphology of Surfside Beach, Texas, after landfall of the 2017 Hurricane Harvey are presented. The results suggested that a noticeable and well-shaped scour runnel and ridge formed in line with the theory and laboratory studies of scour in front of seawalls and breakwaters. Lessons learned include that the scour depths of even less than half a meter may have contributed to the displacement of single boulders of the seawall. While this does not represent major damage, it requires attention with regard to the weak spots when planning for future extreme events. The observations also showed that a combination of site visit (rapidly after the event) and remotely sensed data during the event enables a more comprehensive analysis of the geomorphologic processes. Particularly, satellite-based data can provide information when access to the site is still difficult/dangerous or when investigators may cause an obstruction for first responders. Site visits should be conducted as early as is feasible to avoid large changes of morphology in response to calmer conditions. Finally, a simplified analysis of scour depth confirmed that expressions developed for vertical seawalls and regular breaking waves indeed overpredict the scour depth by orders of magnitude. However, data provided by Sumer and Fredsoe (2000) for rubble-mound breakwaters seemed to provide a reasonable range of values. As in this case, the distance of the scour runnel to the seawall seemed to have a larger potential impact on seawall damage than scour depth. There seems to be a need for expressions to predict not only scour depth but also distance from the seawall more accurately, particularly for a shallow water scenario where the seawall represents the most onshore end of a beach. In general, it should also be highlighted that the seawall in Surfside performed well overall, and experienced limited impacts from this severe event. This is also likely associated with the fact that storm surge and waves were not as severe as they have been in past events, but they may be more severe in future events.

#### ACKNOWLEDGMENTS

The work of the GEER Association is based upon work supported in part by the National Science Foundation through the Geotechnical Engineering Program under Grant No. CMMI-1266418. The GEER Association is made possible by the vision and support of the NSF Geotechnical Engineering Program Directors: Dr. Richard Fragaszy and the late Dr. Cliff Astill. This work was also supported by the National Science Foundation under Grant no. CMMI-1822307. The authors were greatly aided by the briefings and information provided by Jean-Louis Briaud (Texas A&M University, College Station, TX), Marc Ballouz (Institute for Geotechnics & Materials, Austin, TX), and Lee Wooten (GEI Consultants, Woburn, MA). The authors would also like to acknowledge two anonymous reviewers whose comments contributed to the improvement of this article.

# REFERENCES

- Blake, E.S., & Zelinsky, D.A. (2018). "Hurricane Harvey." National Hurricane Center Tropical Cyclone Report AL092017. <a href="https://www.nhc.noaa.gov/data/tcr/AL092017">https://www.nhc.noaa.gov/data/tcr/AL092017</a> Harvey.pdf (August 8, 2018).
- Briaud, J. L., Ting, F. C. K., Chen, H. C., Cao, Y., Han, S. W., & Kwak, K. W. (2001). "Erosion function apparatus for scour rate predictions." *Journal of Geotechnical and Geoenvironmental Engineering*, 127(2), 105-113.
- Briaud, J.L., Govindasamy, A.V., Shafii, I., 2017, "Erosion Charts for Selected Geomaterials." *Journal of Geotechnical and Geoenvironmental Engineering*, 143(10), 04017072.
- Carley, J. T., Coghlan, I. R., Flocard, F., Cox, R. J., & Shand, T. D. (2015). "Establishing the design scour level for seawalls." Proc. of the 22nd Australasian Coastal and Ocean Engineering Conference and the 15th Australasian Port and Harbour Conference, Engineers Australia and IPENZ.
- Connor, C., Campbell, M., Carter, J., & Durnin, T. (2017). "Case Study: Village of Surfside, TX, Design, Performance, and Adaptive Management of Coastal Structures." *Proc. of the Coastal Structures and Solutions to Coastal Disasters Joint Conference 2015*, Boston, Massachusetts.
- Construction Industry Research and Information Association (CIRIA) (1986). Sea walls: Survey of performance and design practice. Technical Note 125.
- DiMarco, S. F., Kelly, F. J., Zhang, J., & Guinasso Jr, N. L. (1995). "Directional wave spectra on the Louisiana-Texas shelf during Hurricane Andrew." *Journal of Coastal Research*, 217-233.
- Figlus, J., Kobayashi, N., Gralher, C., and Iranzo, V. (2011). "Wave Overtopping and Overwash of Dunes." *Journal of Waterway, Port, Coastal, and Ocean Engineering*, 137(1), 26–33.
- Fowler, J. E. (1992). "Scour problems and methods for prediction of scour at vertical seawalls." *U.S. Army Corps of Engineers Coastal Engineering Research Center*, Vicksburg, MS. ADA262140.
- Frost, K.E. (2015). "Hydrodynamic and sedimentary response to tropical storm Bill in the Gulf of Mexico and Christmas Bay." *Master thesis submitted to Texas A&M University*.
- Google Earth (2018a). Image Landsat/Copernicus, image @ Digital Globe, 21 March 2018. (Aug. 7, 2018).



- Google Earth (2018b). Image @ Digital Globe, 22 January 2017. (Aug. 7, 2018).
- Google Earth (2018c). Image @ Digital Globe, 21 March 2015. (Aug. 7, 2018).
- Henry, L. (2017). Video: "Surfside Beach evacuated because of Harvey." Fox 26 Houston News, <a href="https://www.youtube.com/watch?v=hNnbLl\_JCN4">https://www.youtube.com/watch?v=hNnbLl\_JCN4</a>. (Aug. 9 2018).
- Herbich, J. B., & Ko, S. C. (1969). "Scour of sand beaches in front of seawalls." Coastal Engineering, 622-643.
- Kramer, S. L. (1988). "Triggering of liquefaction flow slides in coastal soil deposits." Engineering Geology, 26(1), 17-31.
- Kraus, N. C., & McDougal, W. G. (1996). "The effects of seawalls on the beach: Part I, an updated literature review." *Journal of Coastal Research*, 691-701.
- Lippmann, T. C., & Holman, R. A. (1989). "Quantification of sand bar morphology: A video technique based on wave dissipation." *Journal of Geophysical Research: Oceans*, 94(C1), 995-1011.
- McDougal, W.G., Kraus, N.C., & Ajiwibowo, H. (1996). "The effects of seawalls on the beach: part II, numerical modeling of supertank seawall tests." *Journal of Coastal Research*, 702-713.
- Nederhoff, C. M., Lodder, Q. J., Boers, M., Den Bieman, J. P., & Miller, J. K. (2015). "Modeling the effects of hard structures on dune erosion and overwash: A case study of the impact of Hurricane Sandy on the New Jersey coast." *Proc. of the Coastal Sediments* 2015, San Diego, California, USA.
- NOAA (2019). "Tidal datums" <a href="https://tidesandcurrents.noaa.gov/datum">https://tidesandcurrents.noaa.gov/datum</a> options.html (Feb. 8, 2019).
- Powell, K.A. (1987). "Toe scour at seawalls subject to wave action." HR Wallingford, U.K., Report No. SR119.
- Rodriguez, A. B., Hamilton, M. D., & Anderson, J. B. (2000). "Facies and evolution of the modern Brazos Delta, Texas: wave versus flood influence." *Journal of Sedimentary Research*, 70(2), 283-295.
- Seelig, W.N., & Sorensen, R.M. (1973). "Investigation of shoreline changes at Sargent Beach, Texas." *Texas A&M University Sea Grant*, TAMU-SG-73-212, COE-169, 153.
- Shand, R. D., Bailey, D. G., & Shepherd, M. J. (2001). "Longshore realignment of shore-parallel sand-bars at Wanganui, New Zealand." *Marine Geology*, 179(3-4), 147-161.
- Snedden, J. W., Nummedal, D., & Amos, A. F. (1988). "Storm-and fairweather combined flow on the central Texas continental shelf." *Journal of Sedimentary Research*, 58(4), 580-595.
- Stark, N., Jafari, N., Ravichandran, N., Shafii, I., Smallegan, S., Bassal, P., & Figlus, J. (2017). *The geotechnical aspects of coastal impacts during Hurricane Harvey*, GEER Association Report No. GEER-054.
- Sumer, B. M., & Fredsøe, J. (2000). "Experimental study of 2D scour and its protection at a rubble-mound breakwater." *Coastal Engineering*, 40(1), 59-87.
- Sumer, B.M., and Fredsoe, J. (2002), "The mechanics of scour in the marine environment." World Scientific, New Jersey.
- Tomlinson, R. B., Jackson, A., & Bowra, K. (2016). "Gold Coast Seawall: Status Investigations and Design Review." *Journal of Coastal Research*, 75(1), 715-719.
- Tsai, C. P. (1995). "Wave-induced liquefaction potential in a porous seabed in front of a breakwater." *Ocean Engineering*, 22(1), 1-18.
- Tsai, C. P., Chen, H. B., & You, S. S. (2009). "Toe scour of seawall on a steep seabed by breaking waves." *Journal of Waterway, Port, Coastal, and Ocean Engineering*, 135(2), 61-68.
- TXGLO (2019). "Surfside Shoreline Stabilization." <a href="http://www.glo.texas.gov/coastal-grants/projects/1471-surfside-shoreline-stabilization.html">http://www.glo.texas.gov/coastal-grants/projects/1471-surfside-shoreline-stabilization.html</a> (Feb. 10, 2019).
- Watson, R.L. (2003). "Severe beach erosion at Surfside, Texas, caused by engineering modifications to the coast and the rivers." *TexasCoastGeology.com*, <a href="http://texascoastgeology.com/papers/surfside.pdf">http://texascoastgeology.com/papers/surfside.pdf</a> > (Aug. 13, 2018).
- Wentworth, C. K. (1922). "A scale of grade and class terms for clastic sediments." The Journal of Geology, 30(5), 377-392.
- Whitehouse, R.J.S. (2006). "Scour at coastal structures." *Proc. of the 3rd International Conference on Scour and Erosion*, Amsterdam, the Netherlands.



# The Journal's Open Access Mission is generously supported by the following Organizations:









Access the content of the ISSMGE International Journal of Geoengineering Case Histories at: <a href="https://www.geocasehistoriesjournal.org">https://www.geocasehistoriesjournal.org</a>

Downloaded: Tuesday, November 18 2025, 12:12:02 UTC